Article

Comparative Spectroscopic Investigation of Tm^{3+}:Tellurite Glasses for 2-μm Lasing Applications

Huseyin Cankaya [1,2,3,*], **Adil Tolga Gorgulu** [1], **Adnan Kurt** [4] ⓘ, **Adolfo Speghini** [5] ⓘ, **Marco Bettinelli** [5] ⓘ and **Alphan Sennaroglu** [1,6,*]

[1] Laser Research Laboratory, Departments of Physics and Electrical-Electronics Engineering, Koç University Rumelifeneri, Sariyer, Istanbul 34450, Turkey; agorgulu@ku.edu.tr

[2] Center for Free-Electron Laser Science, Deutsches Elektronen Synchrotron (DESY), Notkestrasse 85, 22607 Hamburg, Germany

[3] Physics Department, University of Hamburg, Luruper Chaussee 149, 22761 Hamburg, Germany

[4] Teknofil. Inc., Zekeriyakoy, Istanbul 34450, Turkey; adnan.kurt@teknofil.com.tr

[5] Dipartimento di Biotecnologie, University of Verona and INSTM UdR Verona, Ca'Vignal, Strada Le Grazie 15, 37134 Verona, Italy; adolfo.speghini@univr.it (A.S.); marco.bettinelli@univr.it (M.B.)

[6] Koç University Surface Science and Technology Center (KUYTAM), Koç University Rumelifeneri, Sariyer, Istanbul 34450, Turkey

[*] Correspondence: huseyin.cankaya@cfel.de (H.C.); asennar@ku.edu.tr (A.S.); Tel.: +49-40-8998-6358 (H.C.); +90-212-338-1429 (A.S.)

Abstract: We performed a comparative spectroscopic analysis on three novel Tm^{3+}:tellurite-based glasses with the following compositions Tm$_2$O$_3$:TeO$_2$-ZnO (TeZnTm), Tm$_2$O$_3$:TeO$_2$-Nb$_2$O$_5$ (TeNbTm), and Tm^{3+}:TeO$_2$-K$_2$O-Nb$_2$O$_5$ (TeNbKTm), primarily for 2-μm laser applications. Tellurite glasses were prepared at different doping concentrations in order to investigate the effect of Tm^{3+} ion concentration as well as host composition on the stimulated emission cross sections and the luminescence quantum efficiencies. By performing Judd–Ofelt analysis, we determined the average radiative lifetimes of the ^{3}H$_4$ level to be 2.55 ± 0.07 ms, 2.76 ± 0.03 ms and 2.57 ± 0.20 ms for the TeZnTm, TeNbTm and TeNbKTm samples, respectively. We clearly observed the effect of the cross-relaxation, which becomes significant at higher Tm$_2$O$_3$ concentrations, leading to the quenching of 1460-nm emission and enhancement of 1860-nm emission. Furthermore, with increasing Tm$_2$O$_3$ concentrations, we observed a decrease in the fluorescence lifetimes as a result of the onset of non-radiative decay. For the ^{3}H$_4$ level, the highest obtained quantum efficiency was 32% for the samples with the lowest Tm$_2$O$_3$ ion concentration. For the 1860-nm emission band, the average emission cross section was determined to measure around 6.33 ± 0.34 × 10^{-21} cm^2, revealing the potential of thulium-doped tellurite gain media for 2-μm laser applications in bulk and fiber configurations.

Keywords: glass lasers; tellurite glass; thulium; thulium-doped laser glasses; solid-state spectroscopy; lanthanide ion-doped glasses; 2-micron lasers

1. Introduction

Thulium-doped systems are drawing a great deal of interest for numerous laser applications in the near and mid-infrared regions of the spectrum, since they provide broad emission bands covering the empty region (1400–2700 nm) between neodymium and erbium systems. In this respect, transitions originating from the ^{3}F$_4$ (^{3}F$_4$→^{3}H$_4$ and ^{3}F$_4$→^{3}H$_5$ transitions corresponding to 1.5-μm and 2.5-μm emissions) and ^{3}H$_4$ (^{3}H$_4$→^{3}H$_6$ transition corresponding to 1.9-μm emissions) energy states are worth studying. For this purpose, we choose to employ a 800-nm excitation scheme, which leads two broad emission bands centered near 1.9 μm and 1.5 μm. Employing this pumping scheme is further beneficial

because there are many commercial pump sources available at these wavelengths and this pumping scheme provides an additional advantage, namely a "two-for-one" process which favors 1.9-μm emission at higher active ion concentrations.

The broad emission band around 1.9 μm can be utilized to build new mid-infrared laser sources suitable for spectroscopic, chemical, and atmospheric sensing applications [1]. In addition, strong water absorption occurs at these wavelengths, making thulium-doped gain media very attractive in the development of lasers for biomedical applications such as tissue welding and ablation [2,3]. Therefore, investigation of novel laser materials, especially thulium-doped hosts which fluoresce around 2 μm, deserves a great deal of attention, considering the ever-increasing demand and need for new laser sources operating in the near- and mid-IR regions of the spectrum.

So far, detailed studies have been conducted on germinate, silicate, and fluoride glass hosts together with various crystal gain media doped with rare earths for 2-μm laser applications [4–6]. Among other laser gain media, tellurite glasses (with network former TeO_2) offer several benefits, such as high chemical stability, easy and low-cost production due to their amorphous nature, and a wide transparency range from 0.355 to 5 μm [3,7,8]. Tellurite glasses are known to be moisture-resistant, thermally and mechanically stable materials, making them attractive for fiber laser applications as well [9,10]. Furthermore, tellurite glass hosts have relatively low phonon energies (700–750 cm^{-1}). Hence, non-radiative decay is relatively low which leads to relatively high luminescence quantum efficiencies.

To date, most of the effort has been spent on Nd^{3+}- and Er^{3+}-doped tellurite glass systems [11–16] and there are relatively fewer studies conducted on the Tm^{3+}-doped tellurite glasses [17–25]. Recently, lasing and mode-locked operation from bulk thulium-doped tellurite glasses were reported [20,26–28]. Since Tm^{3+}-doped tellurite glasses offer a great potential for the development of 2-μm laser sources in bulk as well as fiber configurations, there is interest in further exploring the spectroscopic properties of the tellurite glass hosts doped with thulium.

In this study, we performed a comparative spectroscopic analysis of three different tellurite glasses with various Tm^{3+} concentrations in order to investigate the dependence of the emission cross section and quantum efficiency, which are among the most critical parameters for laser applications. In particular, we studied tellurite glasses with the compositions Tm_2O_3:TeO_2-ZnO, Tm_2O_3:TeO_2-Nb_2O_5, and Tm^{3+}:TeO_2-K_2O-Nb_2O_5. We investigated the influence of doping concentration as well as the host composition, both of which affect the cross relaxation rate and the luminescence quantum efficiency. The analysis was conducted for the two emission bands with peaks at 1460 nm ($^3F_4$ level) and 1860 nm ($^3H_4$ level), and Judd–Ofelt theory was used in the analysis of the experimental data.

2. Experimental Procedure and Analysis

2.1. Experiment

Tellurite-based glass samples doped with Tm_2O_3 were prepared by using the melt quenching technique which was described in our previous study [29]. Three kinds of tellurite-based glass samples were prepared with the glass network modifiers niobium oxide, zinc oxide, and a mixture of potassium and niobium oxide. The Tm_2O_3 concentration was varied between 0.125% and 1%. Two tellurite-based glass samples were prepared by using niobium oxide as a glass modifier: (x)Tm_2O_3-(95)TeO_2-(5-x)Nb_2O_5, (TeNbTm) where x = 1.0 and 0.25 (1.0 and 0.25 mol %); four samples were prepared at different concentrations using zinc oxide as a glass modifier: (x)Tm_2O_3-(80)TeO_2-(20-x)ZnO (TeZnTm), where x = 1.0, 0.5, 0.25 and 0.125 (1.0, 0.5, 0.25 and 0.125 mol %); and four thulium-doped tellurite glasses with potassium and niobium oxide were prepared at different Tm_2O_3 concentrations (x)Tm_2O_3-(70)TeO_2-(15)K_2O-(15)Nb_2O_5 (TeNbKTm) where x = 1.0, 0.5, 0.25 and 0.125 (1.0, 0.5, 0.25 and 0.125 mol %).

The absorption spectra of the glass samples were recorded by using a commercial spectrophotometer. In order to measure the emission spectrum, a home-made, 60-ns pulsed,

tunable Ti:sapphire laser was employed as the excitation source. The emission spectra and lifetime measurements were conducted as described in detail in [29]. All measurements were carried out at room temperature.

2.2. Judd–Ofelt Analysis

In order to study the effect of the Tm^{3+} ion concentration on the radiative lifetimes for the $^3F_4$ and $^3H_6$ levels, Judd–Ofelt (J-O) theory was employed. According to the theory, the effect of the electric-dipole transition from the ground state *SLJ* to an exited state *S'L'J* on the integrated absorption coefficient $\left(\Sigma_\mu\right)_{calc}$ of the rare earth ions can be calculated by using the following equation [30,31],

$$\left(\Sigma_\mu\right)_{calc} = \frac{8\pi^3 e^2}{3ch}\frac{\left(n^2+2\right)^2}{9n}\frac{\overline{\lambda}}{(2J+1)}N_o x \sum_{t=2,4,6} \Omega_t \left|\left\langle SLJ\|U^{(t)}\|S'L'J'\right\rangle\right|^2 \tag{1}$$

Here, N_o is the ion concentration in the gain medium, e is the electron charge, c is the speed of light, h is Planck's constant, n is the refractive index, $\overline{\lambda}$ is the average wavelength of the absorption band, J is the total angular momentum quantum number, the Ω_t's are the J-O intensity parameters, *SLJ* and *S'L'J'* are the ground state and excited state of the dipole transition, respectively, and $U^{(t)}$ is the doubly reduced matrix element of the unit tensor operator. The Ω_t's can be estimated by using the measured integrated absorption coefficient $\left(\Sigma_\mu\right)_{exp}$ and the matrix elements in [32]. $\left(\Sigma_\mu\right)_{exp}$ can be obtained by calculating the integral under the absorption spectrum for each transition Then, Ω_t's can be determined by fitting the experimental integrated absorption coefficient to theoretically calculated value. Then, the spontaneous emission probability $(A(J,J'))$ of the dipole transition from *SLJ* to *S'L'J'* can be calculated by using the equation,

$$A(J,J') = \frac{64\pi^4 e^2}{3h(2J+1)}\frac{n\left(n^2+2\right)^2\overline{v}^3}{9}x\sum_{t=2,4,6}\Omega_t\left|\left\langle SLJ\|U^{(t)}\|S'L'J'\right\rangle\right|^2 \tag{2}$$

In Equation (2), $\overline{v}$ is the average wave number of the corresponding dipole transition. By using the calculated $A(J,J')$ from the *J*th excited state to all possible *J'* states, the radiative lifetime τ_R for the *J*th excited state can be calculated from

$$\tau_R = \frac{1}{\sum\limits_{j} A(J,J')} \tag{3}$$

3. Results and Discussion

3.1. Absorption Spectroscopy

Figure 1a,b shows the energy level diagram and the absorption spectra of two Tm_2O_3:TeO_2-Nb_2O_5 glass samples with Tm_2O_3 concentrations of 1.0 and 0.25 mol % in the range of 450–2050 nm. The other glass samples with different glass modifiers exhibit similar absorption characteristics but different absorption strengths, which will be discussed later. Table 1 summarizes the Ω_t's intensity parameters determined for three different glass hosts with 1 mol % ion concentration by employing J-O theory described above. In the radiative lifetime calculations for the decay from $^3F_4$ and $^3H_4$ levels to the ground state, we only used J-O intensity parameters derived from the absorption spectrum of the 1 mol % doped samples, where the signal to noise ratio is the highest. We also used the fact that the radiative lifetime is independent of active ion concentration. The average radiative lifetimes for the niobium containing glasses were determined as 2.76 ms and 0.37 ms for the sample TeNbTm, and 2.57 ms and 0.35 ms for the sample TeNbKTm. For the glasses containing zinc as a modifier (TeZnTm), we obtained average radiative lifetimes of 2.55 ms and 0.37 ms for the $^3H_4$ and $^3F_4$ levels, respectively.
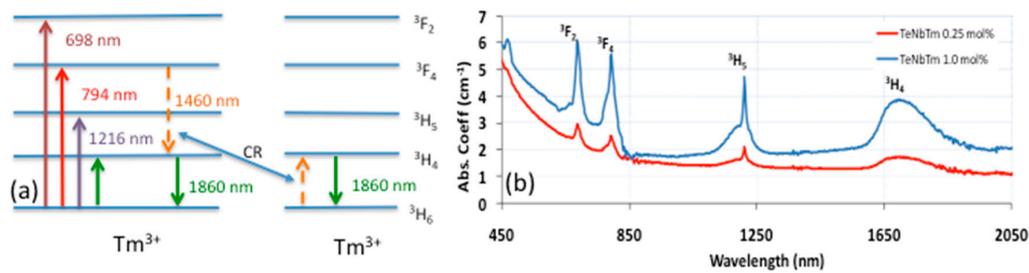
Figure 1. (**a**) Energy level diagram of the Tm^{3+} ion. CR: Cross-relaxation (**b**) Absorption spectra of two Tm_2O_3: TeO_2-Nb_2O_5 glass samples with Tm_2O_3 concentrations of 1.0 and 0.25 mol % in the range of 450–2050 nm. The corresponding absorption bands from the ground state ($^3H_6$) are indicated.

Table 1. Judd–Ofelt (J-O) intensity parameters for three different glass hosts with 1 mol % Tm ion concentration.

J-O Parameters	Ω_2	Ω_4	Ω_6
	$(10^{-20}\ cm^2)$	$(10^{-20}\ cm^2)$	$(10^{-20}\ cm^2)$
TeNbKTm	4.51 ± 0.79	0.76 ± 0.46	1.13 ± 0.67
TeZnTm	4.02 ± 0.56	0.93 ± 0.33	1.12 ± 0.47
TeNbTm	4.09 ± 0.03	0.69 ± 0.01	1.11 ± 0.01

3.2. Emission Spectroscopy and Analysis

Figure 2a shows the fluorescence decay signal of the $^3H_4$ level and $^3F_4$ level, corresponding to the 1860-nm and 1460-nm transitions of the two TeO_2-K_2O-Nb_2O_5 samples with Tm_2O_3 concentrations of 1.0 and 0.125 mol %. The fluorescence signal has a sharp peak following an exponential decay. As can be seen from Figure 2b, the curves corresponding to the 1860-nm transition have a smooth peak in comparison with the other transition. That is mainly due to increase in the population in $^3H_4$ level resulting from the decay from the $^3F_4$ to $^3H_4$ level as illustrated in the energy level diagram in Figure 1a. Similar behavior was observed for the other glass samples with different glass modifiers. In the case of 0.125 mol % doping concentration for the 1860-nm transition (Figure 2b), the fluorescence signal exhibits an initial rise followed by an exponential decay. This can be attributed to the slow decay rate from the $^3F_4$ to $^3H_4$ level, filling the population in the $^3H_4$ level. In the case of the sample with 1.0 mol % doping concentration, this effect is negligible due to the faster decay rate from $^3F_4$ to $^3H_4$. The fluorescence lifetimes (τ_F) were obtained by fitting a single exponential decay curve to the tail of the measured signal, where the cross-relaxation effect is negligible. From the calculated radiative lifetimes and experimentally measured fluorescence lifetimes, the luminescence quantum efficiency (η) can then be determined by using $\eta = \tau_F / \tau_R$.
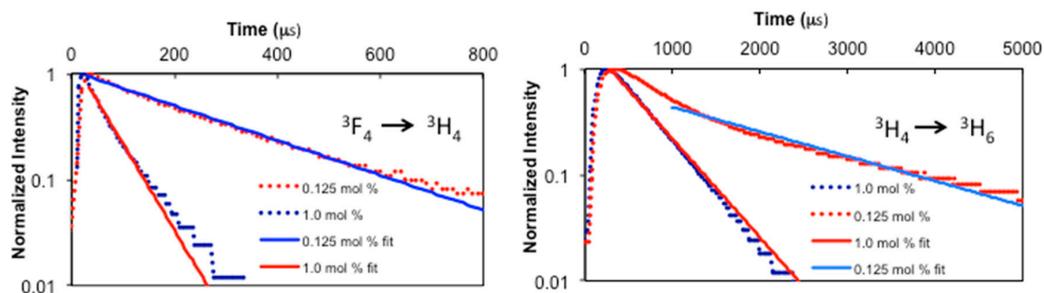

Figure 2. Measured fluorescence decay curves and the exponential fits of the (**a**) $^3F_4$ level and (**b**) $^3H_4$ level for the two Tm_2O_3: TeO_2-K_2O-Nb_2O_5 (TeNbKTm) samples with Tm_2O_3 concentrations of 1.0 and 0.125 mol % [29].

Table 2 summarizes the obtained fluorescence lifetimes and quantum efficiencies of the glass samples for the two transitions peaking at 1860 nm and 1460 nm. With increasing Tm_2O_3 concentration from 0.125 to 1.0 mol %, we observed a decrease in the fluorescence lifetime due to the increasing role of nonradiative relaxation mechanisms. The Te_2O_3-Nb_2O_5 glass with 0.25 mol % Tm_2O_3 doping had the longest fluorescence lifetime (893 μs) for the 1860-nm emission band among the glass samples investigated in this paper. The highest quantum efficiency for the sample TeZnTm was obtained as 32% for the 1860-nm emission band and 89% for the 1460-nm emission band when the ion concentration was 0.125 mol %. We obtained the highest quantum yields of 32% and 76% for the 1860 and 1460 nm emission bands, respectively, in the sample TeNbTm, when the ion concentration was 0.25 mol %.

Table 2. Measured fluorescence lifetimes (τ_F), calculated radiative lifetimes (τ_R), and the corresponding luminescence quantum yields (η) for the two transitions at 1860 nm and 1460 nm.

Fluorescence and Radiative Lifetimes and Quantum Yields	τ_F (μs)		η (%)		$\tau_{Raveraged}$ (ms)	
	$^3H_4$	$^3F_4$	$^3H_4$	$^3F_4$	τ_R (1860 nm)	τ_R (1460 nm)
TeNbKTm [29]	**1860 nm**	**1460 nm**	**1860 nm**	**1460 nm**	**(ms)**	**(ms)**
0.125 mol %	814	258	32	74	2.57	0.35
0.25 mol %	572	199	22	57	-	-
0.5 mol %	545	148	21	43	-	-
1.0 mol %	439	47	17	14	-	-
TeZnTm					τ_R (1860 nm)	τ_R (1460 nm)
0.125 mol %	806	327	32	89	2.55	0.37
0.25 mol %	722	250	28	68	-	-
0.5 mol %	511	171	20	47	-	-
1.0 mol.%	145	35	6	10	-	-
TeNbTm					τ_R (1860 nm)	τ_R (1460 nm)
0.25 mol %	893	284	32	76	2.76	0.37
1.0 mol %	382	76	14	20	-	-

Figure 3a shows the emission spectra of the two transitions of Tm^{3+} ion originating from $^3F_4$ and $^3H_4$ levels to the ground level for the TeZnTm glass host with Tm_2O_3 concentrations of 1.0 and 0.25 mol %. The emission spectra clearly show the two emission bands centered around 1860 nm and 1460 nm and further verify the role of cross relaxation, which is quite common for the Tm^{3+}-doped systems [33,34]. Cross relaxation is a non-radiative energy transfer process, which becomes significant at high ion concentrations, leading to the quenching of the 1460-nm emission and enhancement of the 1860-nm emission band (Figure 3a). On the other hand, the quantum efficiency drops from 32 to 6% for TeO_2-ZnO glass host. As the Tm^{3+} concentration increased, similar enhancement behavior was observed for the other tellurite glass hosts. It is important to find an optimum concentration level here where quantum yield and pump absorption are not dramatically low and still cross-relaxation is significant. Regarding this fact, 0.25 or 0.5 mol % Tm_2O_3-doped samples are potential candidates as hosts in laser applications for bulk as well as fiber applications. Figure 3b shows the emission spectra of the glass hosts with different glass modifiers at 1.0 mol % dopant concentration. As can be seen, the 1460-nm emission band remains similar for different glass modifiers. On the other hand, glass modifier changes produce a notable change in the 1860-nm emission band. In particular, the TeNbKTm glass has the highest emission peak at 1860 nm, whereas the lowest peak of 1795 nm was observed in the TeNbTm host.
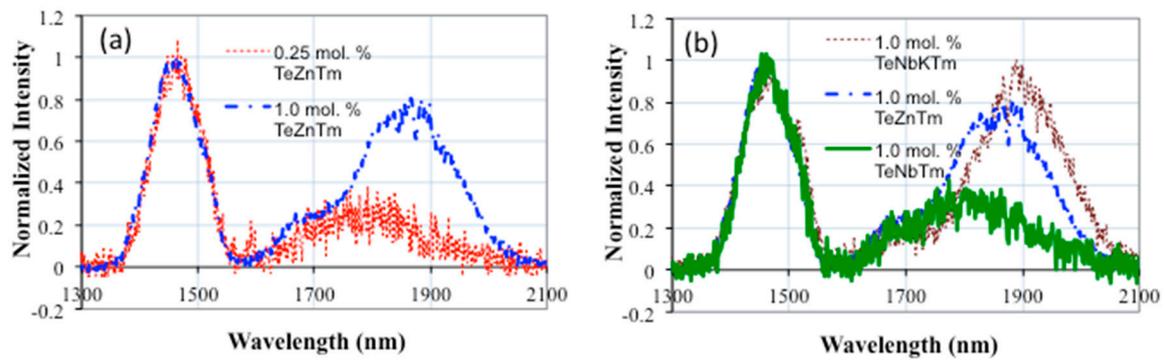
Figure 3. (**a**) Emission spectra of the two transitions of the Tm^{3+} ion originating from $^3F_4$ and $^3H_4$ levels to the ground level for the glass host TeZnTm with Tm$_2$O$_3$ concentrations of 1.0 and 0.25 mol %; (**b**) Emission spectra of the three glass hosts TeNbKTm, TeZnTm and TeNbTm, each with 1.0 mol % Tm$_2$O$_3$ doping.

In order to obtain the emission cross section, we used both the Fuchtbauer–Ladenburg equation [35,36],

$$\sigma_{em}(\lambda) = \frac{\lambda^5 I(\lambda) A(J, J')}{8\pi n^2 c \int I(\lambda)\lambda d\lambda},$$ (4)

and the McCumber formula [37],

$$\sigma_{em}(\lambda) = \sigma_a(\lambda) \left[\frac{Z_l}{Z_u}\right] \exp\left[\frac{hc}{kT}\left(\frac{1}{\lambda_{ZP}} - \frac{1}{\lambda}\right)\right],$$ (5)

where $\sigma_a(\lambda)$ is the absorption cross section, $\left[\frac{Z_l}{Z_u}\right]$ represents the ratio of the parity functions of lower and upper states (13/9 for the Tm^{3+} ion), h is the Planck constant, k is the Boltzmann constant, T is the absolute temperature, and λ_{ZP} is the wavelength of the zero phonon line. From the overlap of the absorption and emission bands, λ_{ZP} was estimated to be 1780 nm. McCumber formalism provides an accurate estimate of the emission cross section as well as its spectral distribution for narrow band emission [38]. On the other hand, the Fuchtbauer–Ladenburg formalism is proven to be accurate for low ion-doping concentrations, where the reabsorption of the emitted photons is negligible and the analysis is applicable to relatively broadband emissions in comparison with the case in McCumber approach, since there is no assumption of the band shape. In Table 3, the emission cross sections obtained by using both formalisms are shown for the two emission bands of the tellurite glasses at different Tm$_2$O$_3$ concentrations. By using the Fuchtbauer–Ladenburg equation for the TeNbTm sample, we obtained average stimulated emission cross section values of $2.62 \pm 0.02 \times 10^{-21}$ and $5.63 \pm 0.02 \times 10^{-21}$ cm^2 for the 1460-nm and 1860-nm bands, respectively. As can be further seen from the table for the sample containing zinc as a glass modifier (TeZnTm), the average emission cross sections were determined to be $2.78 \pm 0.39 \times 10^{-21}$ and $6.33 \pm 0.34 \times 10^{-21}$ cm^2 for the 1460- and 1860-nm bands, respectively. These results compare well with values reported for other tellurite hosts [9,39] and it can also be concluded that for the TeZnTm sample, we obtained higher stimulated emission cross sections (as high as $6.33 \pm 0.34 \times 10^{-21}$ cm^2), especially for the 1860-nm emission band. As can be seen from Table 3, the TeNbKTm glass host has the highest average absorption cross section (8.18×10^{-21} cm^2) among the three hosts, at 794 nm. The TeZnTm glass host also has a reasonably high absorption cross section (7.85×10^{-21} cm^2). Furthermore, at low doping concentration levels, the quantum efficiencies for both transitions are quite high in comparison with the other hosts, suggesting that the TeZnTm glasses are the most promising laser gain media among the materials explored in this study.

Table 3. Emission cross sections and bandwidths at full-wave half maximum (FWHM) of the 1460-nm and 1860-nm bands, and absorption cross sections at 794 nm for the Tm^{3+}:TeO_2-based glass hosts at different Tm_2O_3 concentrations.

	$\Delta\lambda$ (FWHM, nm)		σ_{em} (10^{-21} cm^2)			σ_a (10^{-21} cm^2)
	1460 nm	1860 nm	1460 nm	1860 nm	1860 nm	794 nm
TeNbKTm [29]			Fucht.-Laden.		McCumber	
1.0 mol %	122	170	2.67 ± 0.53	5.61 ± 0.42	6.21	9.07
0.5 mol %	116	231	2.74 ± 0.54	6.12 ± 0.45	6.04	8.33
0.25 mol %	133	319	2.40 ± 0.48	5.46 ± 0.40	5.79	8.26
0.125 mol %	128	240	3.00 ± 0.59	6.85 ± 0.51	6.10	7.07
Average			2.70 ± 0.54	6.01 ± 0.45	6.04 ± 0.18	8.18
TeZnTm						
1.0 mol %	106	192	2.74 ± 0.40	5.48 ± 0.30	6.00	8.08
0.5 mol %	119	200	2.52 ± 0.37	5.65 ± 0.31	5.00	7.79
0.25 mol %	111	172	2.91 ± 0.37	6.85 ± 0.33	4.98	7.65
0.125 mol %	106	200	2.95 ± 0.43	7.36 ± 0.40	5,60	7.89
Average			2.78 ± 0.39	6.33 ± 0.34	5.40 ± 0.5	7.85
TeNbTm						
1.0 mol %	105	237	2.65 ± 0.02	4.99 ± 0.02	5.00	7.68
0.25 mol %	100	103	2.60 ± 0.02	6.28 ± 0.02	6.20	6.90
Average			2.62 ± 0.02	5.63 ± 0.02	5.60 ± 0.85	7.29

As can be seen from Table 3, both formalisms agree reasonably well for all glasses investigated in this study. Figure 4 further shows the absorption and emission cross sections as a function of wavelength for the TeNbKTm samples with 1.0 mol % doping concentration, based on the McCumber analysis. As can be seen, the emission cross section has a broad, smooth peak, which makes the glass system a promising candidate for ultrafast laser applications.
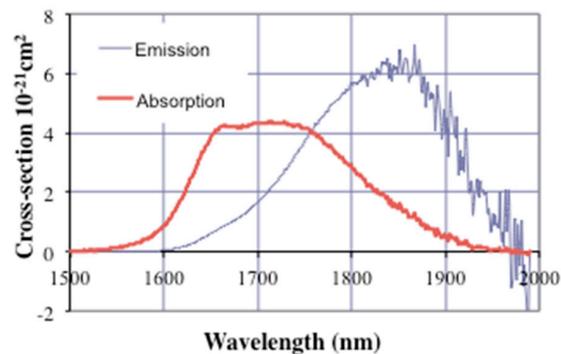
Figure 4. Absorption and emission cross section of the 1.0% Tm_2O_3-doped TeNbKTm samples deduced by using the McCumber analysis.

4. Conclusions

We have conducted a detailed spectroscopic analysis on three new types of tellurite glass materials (Tm_2O_3-TeO_2-ZnO (TeZnTm), Tm_2O_3-TeO_2-Nb_2O_5 (TeNbTm) and Tm_2O_3-TeO_2-K_2O-Nb_2O_5 (TeNbKTm)) in order to investigate the effect of the host composition as well as Tm^{3+} ion concentration on the cross sections and the luminescence quantum efficiencies. From the data, it can be concluded that J-O intensity parameters vary slightly among tellurite glasses with different compositions, as expected. Yet, our calculations showed that for the sample containing zinc as a glass modifier (TeZnTm), we obtained shorter radiative lifetimes for the transition corresponding to the 1860-nm

band. We obtained average radiative lifetimes of 2.55 ± 0.07 ms and 2.76 ± 0.03 ms for the TeZnTm and TeNbTm samples for the $^3H_4$ level.

From the lifetime measurements and the radiative lifetime calculations based on the J-O theory, we determined the luminescence quantum efficiencies of the samples. The highest quantum efficiency for the sample TeZnTm was 32% for the 1860-nm emission band and 89% for the 1460-nm emission band. For the sample TeNbTm, we obtained the highest quantum yields as 32% and 76% for the 1860-nm and 1460-nm emission bands, respectively. For higher doping concentrations, we observed a cross-relaxation effect, which enhanced the 1860-nm emission band. Samples with low concentration provide higher quantum efficiencies that are favorable for lasing applications but on the other hand, exhibit weak absorption. When the ion concentration is increased, quantum efficiencies decrease but the absorption near 800 nm together with the cross relaxation effect enhancing the 1860 nm band increase, which suggests that 0.25 or 0.5 mol % samples are potential candidates as hosts in laser applications for bulk as well as fiber applications.

For the TeNbTm sample, we obtained average emission cross sections of $2.62 \pm 0.02 \times 10^{-21}$ and $5.63 \pm 0.02 \times 10^{-21}$ cm^2 for the 1460-nm and 1860-nm bands, respectively. For the sample containing zinc as a glass modifier (TeZnTm), the average emission cross sections were determined to be $2.78 \pm 0.39 \times 10^{-21}$ and $6.33 \pm 0.39 \times 10^{-21}$ cm^2 for the 1460-nm and 1860-nm bands, respectively. These results compare well with values reported for other tellurite hosts [9,39] and it can also be pointed out that for the TeZnTm sample, we obtained higher stimulated emission cross sections, especially for the 1860-nm emission band. Among the hosts we analyzed, TeZnTm glass stands as a good candidate for the development of 2-µm lasers with high emission cross sections near 1860 nm.

References

1. Carrig, T.J.; Hankla, A.K.; Wagner, G.J.; Rawle, C.B.; Kinnie, I.T.M. Tunable Infrared Laser Sources for Dial. In Proceedings of the SPIE Laser Radar Technology and Applications VII, AEROSENSE 2002, Orlando, FL, USA, 1–5 April 2002; pp. 147–155.
2. Bilici, T.; Tabakoglu, H.O.; Topaloglu, N.; Kalaycioglu, H.; Kurt, A.; Sennaroglu, A.; Gulsoy, M. Modulated and continuous-wave operations of low-power thulium (Tm:YAP) laser in tissue welding. *J. Biomed. Opt.* **2010**, *15*, 038001. [CrossRef] [PubMed]
3. Wang, J.S.; Snitzer, E.; Vogel, E.M.; Sigel, J.G.H. 1.47, 1.88, and 2.8 µm emission of Tm^{3+} and Tm^{3+}-Ho^{3+}-codoped tellurite glasses. *J. Lumin.* **1994**, *60*, 145–149. [CrossRef]
4. McAleavey, F.J.; O'Gorman, J.; Donegan, J.F.; MacCraith, B.D.; Hegarty, J.; Maze, G. Narrow linewidth, tunable Tm—Doped fluoride fiber laser for optical-based hydrocarbon gas sensing. *IEEE J. Sel. Top. Quantum Electron.* **1997**, *3*, 1103–1111. [CrossRef]
5. Tsanga, Y.H.; Colemana, D.J.; King, T.A. High power 1.9 µm Tm^{3+}-silica fibre laser pumped at 1.09 µm by a Yb^{3+}-silica fibre laser. *Opt. Commun.* **2004**, *231*, 357–364. [CrossRef]
6. Wu, J.F.; Yao, Z.D.; Zong, J.; Jiang, S.B. Highly efficient high-power thulium-doped germanate glass fiber laser. *Opt. Lett.* **2007**, *32*, 638–640. [CrossRef] [PubMed]
7. Wang, J.S.; Vogel, E.M.; Snitzer, E. Tellurite glass: A new candidate for fiber devices. *Opt.Mater.* **1994**, *3*, 187–203. [CrossRef]
8. Yamane, M.; Asahara, Y. *Glasses for Photonics*; Cambridge University Press: Cambridge, UK, 2000.

9. Kalaycioglu, H.; Cankaya, H.; Cizmeciyan, M.N.; Sennaroglu, A.; Ozen, G. Spectroscopic investigation of Tm^{3+}:TeO$_2$-WO$_3$ glass. *J. Lumin.* **2008**, *128*, 1501–1506. [CrossRef]

10. Zou, X.L.; Toratani, H. Spectroscopic properties and energy transfers in Tm^{3+} singly- and Tm^{3+}/Ho^{3+} doubly-doped glasses. *J. Non Cryst. Solids* **1996**, *195*, 113–124. [CrossRef]

11. Azkargorta, J.; Iparraguirre, I.; Balda, R.; Fernández, J. On the origin of bichromatic laser emission in Nd^{3+}-doped fluoride glasses. *J. Non Cryst. Solids* **2008**, *16*, 11894–11906.

12. Lei, N.; Xu, B.; Jiang, Z.H. Ti:Sapphire laser pumped nd:Tellurite glass laser. *Opt. Commun.* **1996**, *127*, 263–265. [CrossRef]

13. Mori, A.; Sakamoto, T.; Kobayashi, K.; Shikano, K.; Oikawa, K.; Hoshino, K.; Kanamori, T.; Ohishi, Y.; Shimizu, M. 1.58 um broad-band erbium-doped tellurite fiber amplifier. *J. Lightwave Technol.* **2002**, *20*, 794. [CrossRef]

14. Wang, J.S.; Machewirth, D.P.; Wu, F.; Snitzer, E.; Vogel, E.M. Neodymium-doped tellurite single-mode fiber laser. *Opt. Lett.* **1994**, *19*, 1448–1449. [CrossRef] [PubMed]

15. Kalaycioglu, H.; Cankaya, H.; Ozen, G.; Ovecoglu, L.; Sennaroglu, A. Lasing at 1065 nm in bulk Nd^{3+}-doped telluride-tungstate glass. *Opt. Commun.* **2008**, *281*, 6056–6060. [CrossRef]

16. Cankaya, H.; Sennaroglu, A. Bulk Nd^{3+}-doped tellurite glass laser at 1.37 μm. *Appl. Phys. B Lasers Opt.* **2010**, *99*, 121–125. [CrossRef]

17. Li, K.; Zhang, G.; Hu, L. Watt-level 2 μm laser output in Tm^{3+}-doped tungsten tellurite glass double-cladding fiber. *Opt. Lett.* **2010**, *35*, 4136–4138. [CrossRef] [PubMed]

18. Richards, B.; Tsang, Y.; Binks, D.; Lousteau, J.; Jha, A. 2 μm Tm^{3+}/Yb^{3+}-Doped Tellurite Fibre Laser. In Proceedings of the 5th International Conference on Optical, Optoelectronic and Photonic Materials and Applications, London, UK, 29 July–3 August 2007; pp. 317–320.

19. Tsang, Y.; Richards, B.; Binks, D.; Lousteau, J.; Jha, A. Tm^{3+}/Ho^{3+} codoped tellurite fiber laser. *Opt. Lett.* **2008**, *32*, 1282–1284. [CrossRef]

20. Richards, B.; Shen, S.; Jha, A.; Tsang, Y.; Binks, D. Infrared emission and energy transfer in Tm^{3+}, Tm^{3+}-Ho^{3+} and Tm^{3+}-Yb^{3+}-doped tellurite fibre. *Opt. Express* **2007**, *15*, 6546–6551. [CrossRef] [PubMed]

21. Debnath, R.; Bose, S. A comprehensive phononic sof phonon assisted energy transfer in the Yb^{3+} aided upconversion luminescence of Tm^{3+} and Ho^{3+} in solids. *J. Lumin.* **2015**, *161*, 103–109. [CrossRef]

22. Ma, Y.; Wang, X.; Zhang, L.; Huang, F.; Hu, L. Increased radiative lifetime of Tm3+:^{3}F$_4$ ^{3}H$_6$ transition in oxyfluoride tellurite glass. *Mater. Res. Bull.* **2015**, *64*, 262–266. [CrossRef]

23. Wang, W.C.; Zhang, W.J.; Li, L.X.; Liu, Y.; Chen, D.D.; Qian, Q.; Zhang, Q.Y. Spectroscopic and structural characterization of barium tellurite glass fibers for mid-infrared ultra-broad tunable fiber lasers. *Opt. Mater. Express* **2016**, *6*, 2095–2107. [CrossRef]

24. Shen, L.; Cai, M.; Lu, Y.; Wang, N.; Huang, F.; Xu, S.; Zhang, J. Preparation and investigation of Tm^{3+}/Ho^{3+} co-doped germanate-tellurite glass as promising materials for ultrashort pulse laser. *Opt. Mater.* **2017**, *67*, 125–131. [CrossRef]

25. Zhou, D.; Bai, X.; Zhou, H. Preparation of Ho^{3+}/Tm^{3+} co-doped lanthanum tungsten germanium tellurite glass fiber and its laser performance for 2.0 μm. *Sci. Rep.* **2017**, *7*, 44747. [CrossRef] [PubMed]

26. Fusari, F.; Vetter, S.; Lagatsky, A.A.; Richards, B.; Calvez, S.; Jha, A.; Dawson, M.D.; Sibbett, W.; Brown, C.T.A. Tunable laser operation of a Tm^{3+}-doped tellurite glass laser near 2 μm pumped by a 1211 nm semiconductor disk laser. *Opt. Mater.* **2010**, *32*, 1007–1010. [CrossRef]

27. Fusari, F.; Lagatsky, A.A.; Richards, B.; Jha, A.; Sibbett, W.; Brown, C.T.A. Spectroscopic and lasing performance of Tm^{3+}- doped bulk tzn and tzng tellurite glasses operating around 1.9 μm. *Opt. Express* **2008**, *16*, 19146–19151. [CrossRef] [PubMed]

28. Fusari, F.; Lagatsky, A.A.; Jose, G.; Calvez, S.; Jha, A.; Dawson, M.D.; Gupta, J.A.; Sibbett, W.; Brown, C.T.A. Femtosecond mode-locked Tm^{3+} and Tm^{3+}-Ho^{3+} doped 2 μm glass lasers. *Opt. Express* **2010**, *18*, 22090–22098. [CrossRef] [PubMed]

29. Tolga Gorgulu, A.; Cankaya, H.; Kurt, A.; Speghini, A.; Bettinelli, M.; Sennaroglu, A. Spectroscopic characterization of Tm^{3+}:TEO$_2$-K$_2$O-Nb$_2$O$_5$ glasses for 2-μm lasing applications. *J. Lumin.* **2012**, *132*, 110–113. [CrossRef]

30. Judd, B.R. Optical absorption intensities of rare-earth ions. *Phys. Rev.* **1962**, *127*, 750–761. [CrossRef]

31. Ofelt, G.S. Intensities of crystal spectra of rare-earth ions. *J. Chem. Phys.* **1962**, *37*, 511. [CrossRef]

32.   Kaminskii, A.A. *Laser Crystals*; Springer: Berlin, Germany, 1990.

33.   Gebavi, H.; Milanese, D.; Balda, R.; Chaussedent, S.; Ferrari, M.; Fernandez, J.; Ferraris, M. Spectroscopy and optical characterization of thulium doped TZN glasses. *J. Phys. D Appl. Phys.* **2010**, *43*, 13. [CrossRef]

34.   Sennaroglu, A.; Kabalci, I.; Kurt, A.; Demirbas, U.; Ozen, G. Spectroscopic properties of Tm^{3+}:TeO_2-PbF_2 glasses. *J. Lumin.* **2006**, *116*, 79–86. [CrossRef]

35.   Moulton, P.F. Spectroscopic and laser characteristics of ti-Al_2O_3. *J. Opt. Soc. Am. B Opt. Phys.* **1986**, *3*, 125–133. [CrossRef]

36.   Sudesh, V.; Goldys, E.M. Spectroscopic properties of thulium-doped crystalline materials including a novel host, $La_2Be_2O_5$: A comparative study. *J. Opt. Soc. Am. B Opt. Phys.* **2000**, *17*, 1068–1076. [CrossRef]

37.   McCumber, D.E. Einstein relations connecting broadband emission and absorption spectra. *Phys. Rev.* **1964**, *136*, A954. [CrossRef]

38.   Digonnet, M.J.F.; Murphy-Chutorian, E.; Falquier, D.G. Fundamental limitations of the mccumber relation applied to er-doped silica and other amorphous-host lasers. *IEEE J. Quantum Electron* **2002**, *38*, 1629–1637. [CrossRef]

39.   Sennaroglu, A.; Kurt, A.; Özen, G. Effect of cross relaxation on the 1470 and 1800 nm emissions in Tm^{3+}:TeO_2-$CdCl_2$ glass. *J. Phys. Condens. Matter* **2004**, *16*, 2471–2478. [CrossRef]